Real-Time Rate Distortion Optimized and Adaptive Low Complexity Algorithms for Video Streaming

Ahmed Abdelhadi[*], Andreas Gerstlauer[†] and Sriram Vishwanath[†]
[*]University of Houston, Houston, TX
[†]University of Texas at Austin, Austin, TX

Abstract—**Mobile cyberphysical systems provide a platform where communication, computing and control are integrated together. With the increase in the usage of Internet of Things (IoT) devices, it is important to understand the complex interaction between these three subsystems. This paper aims to address this challenge in the context of video delivery over an autonomous aerial vehicle (AAV) network. This network suffers from limited bandwidth and delay constraints of real-time video streaming under time-varying wireless channel conditions. Additionally, it experiences limitations in power consumption and computational complexity due to the embedded system platform running the video transmission protocols. Hence, we design a low complexity real-time video transmission protocols that are suitable for such platforms. In this paper, we provide a comparison between different transmission protocols we developed with respect to temporal and spatial video distortion metrics.**

Index Terms—**Multimedia Networks, Rate-Distortion Optimization, Cyberphysical Systems**

I. INTRODUCTION

Due to the increase in the usage of cyberphysical system devices, there is a need to integrate communication, control and computing resulting in many research challenges. Many applications require reliable control and distribution coupled with high bandwidth communication. Moreover, these systems often operate in an enviroment with limited resources, e.g. computation and power constrained. In this paper, we design and analyze a cyberphysical system that consists of a network of AAVs. This system has multitude of applications in the civilian and military arenas. This work mainly focuses on developing wireless video transmission protocols that are efficient given the stringent constraints of mobile cyberphysical systems [1]–[16]. Such systems are in general characterized by delay sensitivity coupled with the high bandwidth requirement and high computational complexity. These characteristics cause significant video delivery and reliability challenges. The main factors that cause real-time video delviery challenges are high data rate, real-time constraints, and dependencies between frames [17]–[19]. Schedulers for quality of service (QoS) improvement were proposed in [20]–[28] applied to different standards [29]–[33].

Real-time applications, such as video transmissions, are the main focus in this paper. In the past, researchers have mainly investigated delay-tolerant applications [34], [35] for schedulers design [36]–[42] with optimality [43]–[46]. Nowadays, real-time applications are the primary focus of research given all the recent applications on smart phones that require real-time performance, either with approximate solutions [47]–[49] or optimal ones [50]–[58]. Given the bandwidth requirements of real-time applications additional spectrum was recommended in [59]–[67] for designing schedulers [68]–[72] with optimality [73]–[77]. One of the spectrum mainly considered for carrier aggregation is the radar band [78]–[86].

Our goal in this paper is to develop low complexity rate distortion optimized (RDO) and adaptive streaming algorithms to efficiently deliver multimedia over an AAV network called Horus. Our developed transmission techniques minimize the video distortion given the limitation of wireless channels. The developed low-complexity RDO (LCRDO) algorithms outperform conventional video transmission protocols.

A. Our Contributions

Our contributions on the implementation side are summarized as:

- We implement a real-time RDO transmission algorithm that requires a smaller memory and less computational power suitable for real-setting and real-time execution.
- We implement an adaptive transmission algorithm using MPEG2 video compression that minimizes drops when compared to non-adaptive transmission.
- We implement an adaptive MJPEG transmission algorithm that decreases frame drops.

II. RATE-DISTORTION OPTIMIZATION PROBLEM

The goal of the RDO problem is to optimize the amount of distortion in a network for a given rate, where distortion is the degradation is media quality as packets are dropped and rate is the amount of data (i.e. number of packets transmitted per unit time). In [2], an algorithm for minimizing distortion D for a given rate R is shown. The authors solve the RDO problem by minimizing the Lagrangian $D + \lambda R$ where λ Lagrange multiplier. This algorithm is suitable for off-line computation. The problem is defined and solved for every data unit l, i.e. video packet, and so there exist a Lagrange multiplier λ_l for every data unit. Depending on the expected channel rate, the value λ_l is a packet threshold above which the packet is transmitted and below which the packet is not transmitted. Solving the rate distortion optimization problem for every video packet is not efficient for embedded applications in real-time as the transmission policy computation for every packet threshold λ_l is time consuming and hence requires off-line computation. In addition, solving rate-distortion optimization problem presented in [2] requires a mathematical
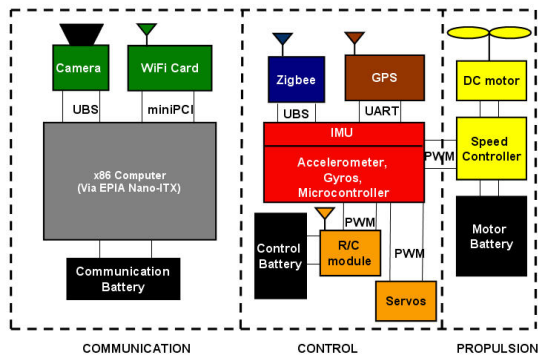
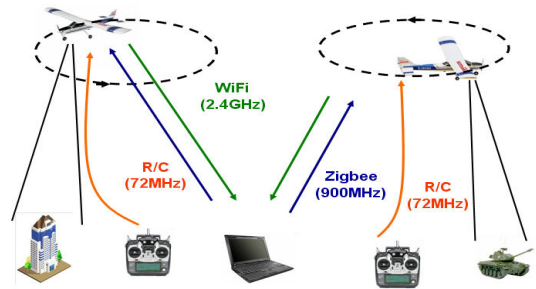Fig. 1. AAV block diagram of internal components

Fig. 2. Horus testbed diagram for two AAVs multiple unicast scenario

Fig. 3. Map of the actual site used for running Horus testbed experiment. The internal circle shows the AAV flight path. The outer circle shows the viewing area of the camera attached to the AAV.

channel model with parameters that are updated regularly if used in real-time systems. This will certainly add more computational complexity to the system. Instead of using a mathematical channel model, we measure channel state by using measurable physical quantities that are already available by default during system operation and therefore will not need additional computation. We use MAC layer beacons[1]. For 802.11 wireless networks, the destination sends beacons to the source periodically by default. These beacons are used in our algorithm at the source to measure the channel state. Hence, our proposed RDO algorithms are characterized by real-time execution where policy/channel state is computed on-line, and low computational complexity.

III. TESTBED

For our experiment, we use Horus AAV node, see section III-A for node description, that are flying in a pre-specified path, see section III-B for the proposed topology. In this experiment, AAVs are streaming video data in real-time to destinations (a laptop is used as a fixed access point). The flight path is chosen to ensure the time-varying nature of wireless channel is significant in the experiment.

The routing path is given a priori and the topology of the network is fixed throughout the experiment. However the nodes are moving in a fixed circular path as described in section III-B. This continuous movement ensures the time-varying nature of wireless channel and reveals the effectiveness of the implemented algorithms.

A. AAV Node Description

The aerial nodes (AAV)that form the network for our experiment include the components shown in Figure 1[2]. These components are Via EPIA Nano-ITX [87] (a x86 computer), Atheros wireless card [88] (for IEEE 802.11 2.4 GHz communications), Zigbee [89] (IEEE 802.15 900 MHz frequency

band for way point navigation) IMU[3] [90] (for controlling the AAV flight), GPS[4] [91] (for location measurement), Remote Control Unit [92] (R/C module uses 72 MHz frequency band for manual flight control), Servo motors [93] (control AAV flaps and rudder) DC motor [94] (moving force of AAV propeller), and a camera (for video capturing). The block diagram is divided into three sections propulsion, control, and communication as shown in Figure 1. Figure 2 shows the wireless connections between AAVs and group access point (laptop).

B. Network Topology

In our experiment, we consider two main network topologies. First, unicast network topology is considered where the AAV transmits to a ground access point (i.e. laptop). The circular path of the AAV is shown in Figure 3. The AAV records live video of the landscape beneath it and transmits this video to the ground access point (laptop). Second, multiple unicast network topology is constructed by two AAV flying in a two different circular paths as shown in Figure 2 recording live video and transmitting to a ground access point (i.e. laptop).

C. Distortion Measure

We consider two metrics of distortion for comparing between various transmission protocols. These metrics are:

---

[1]Periodically, access points broadcast a beacon, and the radio network interface card (NIC) receives these beacons while scanning and takes note of the corresponding signal strengths. The beacons contain information about the access point, including service set identifier (SSID), supported data rates, etc.

[2]UART, PWM, and USB stands for Universal Asynchronous Receiver/Transmitter, Pulse-Width Modulation, and Universal Serial Bus, respectively

[3]IMU stands for Inertial Measurement Unit

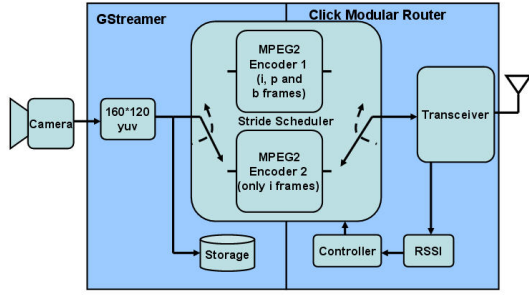[4]GPS stands for Global Positioning System

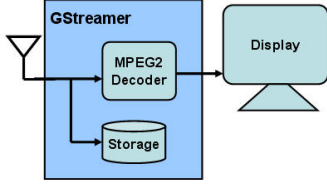Fig. 4. Block diagram of the LCRDO-Beacon algorithm at the transmitter

Fig. 5. Block diagram of the LCRDO-Beacon algorithm at the receiver

1) Temporal Distortion:: It represents the difference between the transmitted video duration from the AAV(s) and the received video duration at the access point (i.e. laptop). So, it is a measure of packet drops during transmission.

2) Spacial Distortion:: For spacial distortiion, we use Structural SIMilarity (SSIM) [95] index of the frames successfully reconstructed at the access point (laptop). The SSIM index is a metric of similarity between distortion-free image (reference image) and distorted image. Hence, it is a measure of perceived image quality. The SSIM index between two windows x and y of common size $N \times N$ is:

$$SSIM(x,y) = \frac{(2\mu_x\mu_y + c_1)(2\sigma_{xy} + c_2)}{(\mu_x^2 + \mu_y^2 + c_1)(\sigma_x^2 + \sigma_y^2 + c_2)} \quad \text{(III.1)}$$

where μ_x and μ_y are the averages of x and y, respectively, σ_x^2 and σ_y^2 are the variances of x and y, respectively, σ_{xy} is the covariance of x and y, and c_1 and c_2 are two stabilizing variables.

IV. VIDEO TRANSMISSION PROTOCOLS

For implementing our transmission protocols, we use Linux operating System (Ubuntu), Click Modular Router open source network stack [96] for implementing our transmission algortihms, and GStreamer open source multimedia framework [97] for video compression.

A. LCRDO-Beacon Algorithm

The low complexity RDO (LCRDO)-Beacon algorithm, used in our implementation, has low computational complexity. The reason for this reduction of computational complexity is high computational demands of MPEG2 video encoding, which requires most of the computational power of Via EPIA computer. The use of beacons for channel state measurement ensure a more reliable real-time performance and concurrently show significant improvement in the general performance with

---

Algorithm 1 LCRDO-Beacon Algorithm

loop
    transmit packets received from the selected/active encoder
    if transceiver receives a beacon **then**
        if $RSSI < X_1$ **then**
            Clear $Queue1$ and $Queue2$ {Ensures real-time delivery}
            Switch to Encoder 2 (i frames only)
        else
            if $RSSI > X_2$ **then**
                Clear $Queue1$ and $Queue2$ {Ensures real-time delivery}
                Switch to Encoder 1 (i, p and b frames)
            end if
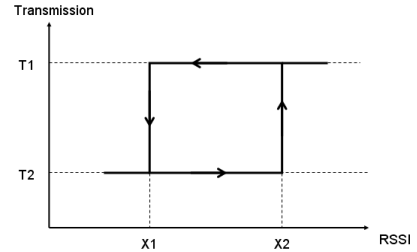   **end if**
    end if
end loop

Fig. 6. Hysteresis: Controller switches to Encoder 2 when RSSI is less than X_1 and to Encoder 1 when RSSI is greater than X_2. No change is done when RSSI is between X_1 and X_2.

respect to unoptimized methods, as will be shown in section IV-D.

The block diagram of the transmitter is shown in Figure 4. The camera driver outputs raw video, which is resized to 160x120 (without loss of generality, this resolution is chosen to minimize the computation on the Via EPIA computer; the algorithm applies equally for higher resolutions). A stride scheduler chooses between different parameters for encoding the raw video into an MPEG2 stream. We use two different encoders:

1) MPEG2 encoder with GOF[5]=5 and an overall frame rate of 25 frames per second (f/s). This corresponds to sending i, p and b frames with an i frame rate of 5 f/s.
2) MPEG2 encoder with GOF=1 and an overall frame rate of 5 f/s. This corresponds to sending i frames only at a rate of 5 f/s.

In this RDO architecture, packets of p and b frames of a single and fixed MPEG2 encoder (running at 25 f/s) are selectively dropped depending on the chosen transmission policy. An equivalent implementation that alternates between

---

[5]Group Of Frames (GOF) is the group of video frames that starts by an i frame then proceeded by p and b frames only. The MPEG video file is a sequence of GOFs; e.g. GOF=5 has one i frame and four p and b frames, while GOF=1 has only i frames and no p and b frames.
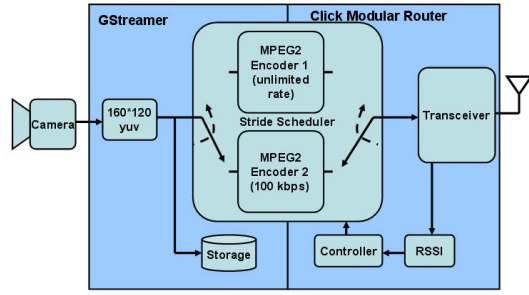
Fig. 7. Block diagram of the LCRDO-Adaptive algorithm for MPEG2 at the transmitter.

Fig. 8. Block diagram of the LCRDO-Adaptive algorithm for MPEG2 at the receiver.

two separate encoders as controlled by a stride scheduler was chosen due to limitations of the GStreamer-internal architecture.

The two outputs of the two MPEG2 compression and packet selection blocks are fed to the transmitter via two queues, $Queue1$ and $Queue2$. These queues are not drawn to simplify the block diagram. For later comparison purposes, a high quality reference copy of the original video is stored in compressed MPEG2 form (with GOF=5 and 25 f/s) using GStreamer. Inside the Click Modular Router, a transceiver realizes wireless transmission of encoded videos and wireless reception of signal strength beacons. The beacons received in the transceiver are passed through a Received Signal Strength Indicator (RSSI[6]) block that decodes the RSSI value and passes it on to a controller block. Finally, the controller block determines packet selection and controls the stride scheduler by executing Algorithm 1.

In the LCRDO-Beacon algorithm (Algorithm 1), the controller switches to the Encoder 2 (i frames only) in the video compression block whenever the RSSI drops below a value X1. Likewise, if the RSSI rises above a value X2, the controller switches to select the Encoder 1 (i, p and b frames) in the video compression block. This hysteresis is shown in Figure 6. In the switching instant, all the contents of $Queue1$ and $Queue2$ are cleared. This is done to avoid sending any residual packets in the queue when switching back and forth between the different encoding modes, ensuring reliable real-time performance.

The block diagram of the receiver is shown in Figure 5. The received signal is decoded using a standard MPEG2 decoder and displayed on the monitor of the ground access point (laptop). At the same time, the received video is stored in compressed MPEG2 format for later analysis.

B. LCRDO-Adaptive Algorithm for MPEG2

In addition to selectively dropping packets, a generalized method for performing RDO and improving the received video quality is to co-design RDO-type packet selection with adaptive video encoding. In such an approach, the video encoding rate is adjusted to the transmission rate in a distortion-optimized way. In addition to improving video quality, adapt-

6The Atheros based card returns an RSSI value of 0 to 127 (0x7f) with 128 (0x80) indicating an invalid value.
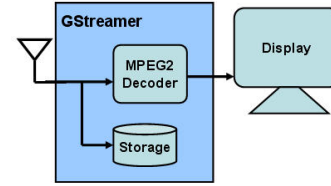
ing encoding parameters to rate variations can significantly reduce average computational requirements in the real-time video encoder. Similar to the LCRDO-Beacon algorithm, such an adaptive approach has an operating mechanism in which the video encoder switches between different modes. Both algorithms require predetermined thresholds used in a hysteresis (see Figure 6). In the LCRDO-Beacon algorithm, the channel state measurement determines when to transmit both independent and dependent or when to drop dependent and only transmit independent frames. By contrast, for the adaptive algorithm, the channel state measurements determine when to transmit video at high quality, i.e. with high bit rate, and when to transmit video at low quality, i.e. with lower bit rate. Both algorithms require channel state measurements and seek to minimize distortion and maximize video quality. The block

---

Algorithm 2 LCRDO-Adaptive Algorithm for MPEG2

loop
    transmit packets received from the selected/active encoder
    if transceiver receives a beacon **then**
        if $RSSI < X_1$ **then**
            Clear $Queue1$ and $Queue2$ {Ensures real-time delivery}
            Switch to Encoder 2 (100 kbps)
        else
            if $RSSI > X_2$ **then**
                Clear $Queue1$ and $Queue2$ {Ensures real-time delivery}
                Switch to Encoder 1 (unlimited rate)
            end if
        end if
    end if
end loop

---

diagram of the low complexity RDO with adaptive co-design (LCRDO-Adaptive) algorithm for MPEG2 transmissions is show in Figure 7. The block diagram is similar to the block diagram of LCRDO-Beacon with the exception that the stride scheduler allows choosing between two different MPEG2 encoders for video compression:

1) MPEG2 encoder with 5 frames per GOF, a frame rate of 25 f/s, and unlimited bit rate.
2) MPEG2 encoder with 5 frames per GOF, 25 f/s frame rate, and 100 kbps transmission rate.

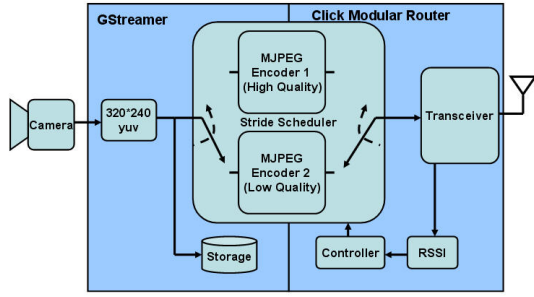The controller block determines packet selection and controls

Fig. 9. Block diagram of the LCRDO-Adaptive algorithm for MJPEG/SMOKE at the transmitter.
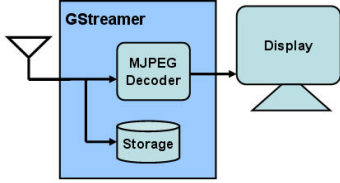

Fig. 10. Block diagram of the LCRDO-Adaptive algorithm for MJPEG/SMOKE at the receiver.

the stride scheduler by executing Algorithm 2. The block diagram of the receiver is shown in Figure 8, which is similar to the LCRDO-Beacon receiver.

Algorithm 3 LCRDO-Adaptive Algorithm MJPEG/SMOKE

loop
  transmit packets received from the selected/active encoder
  if transceiver receives a beacon **then**
    if $RSSI < X_1$ **then**
      Clear $Queue1$ and $Queue2$ {Ensures real-time delivery}
      Switch to Encoder 2 (low quality)
    else
      if $RSSI > X_2$ **then**
        Clear $Queue1$ and $Queue2$ {Ensures real-time delivery}
        Switch to Encoder 1 (high quality)
      end if
    end if
  end if
end loop

C. LCRDO-Adaptive Algorithm for MJPEG/SMOKE

The attractive property of motion JPEG (MJPEG) video compression is the very low computational complexity compared to MPEG2 video compression. This comes at the expense of lower compression leading to higher bandwidth requirements. Furthermore, MJPEG compression is characteristic by all frames being independent, whereas MPEG2 compression has both independent and dependent frames. A variant of MJPEG compression is the SMOKE codec [98], which includes both JPEG frames and delta frames. JPEG
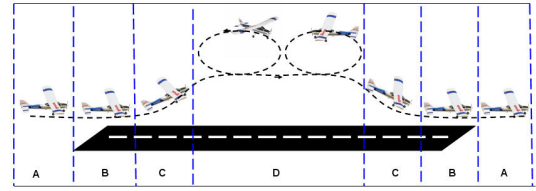

Fig. 11. Flight phases used to calculate average SSIM index

frames are key-frame that are each followed by $N - 1$ delta frames. JPEG frames are independent while delta frames are constructed according to a motion estimation threshold using the key-frame. This threshold specifies how much each 16x16 block of pixels may differ before a new block is generated. A large value of the threshold causes more blocks to stay the same for more frames, decreasing bandwidth usage, but producing less accurate output. Likewise, a small number of delta frames between key-frames increase received video quality at the cost of a higher bit rate, and vise versa. The block diagram of the LCRDO-Adaptive for MJPEG/SMOKE transmitter is show in Figure 9. The camera driver outputs raw video which is resized to 320x240 with frame rate of 10 f/s. A stride scheduler chooses between different parameters for encoding the raw video into an MJPEG/SMOKE stream. We realize two different encoders:

1) MJPEG/SMOKE encoder with high JPEG image quality of 80% and N=8.
2) MJPEG/SMOKE encoder with low JPEG image quality of 30% and N=8.

The rest of the block diagram is similar to the block diagram of LCRDO-Beacon with difference in the controller and the storage blocks. The controller block determines packet selection and controls the stride scheduler by executing Algorithm 3. The storage block stores high quality MJPEG/SMOKE compressed video (with JPEG image quality of 80%, N=8 and 10 f/s) as reference for later analysis. The block diagram of the receiver is shown in Figure 10. The received signal is decoded using MJPEG/SMOKE decoder and displayed on the monitor of the ground station (laptop). At the same time, the received compressed video is stored as MJPEG/SMOKE format for later analysis.

D. Results

We run the flight experiment at Lester Field [99] in Austin, Texas, shown in Figure 3 (the map is taken from Google maps). In the flight experiment, the AAV records live video of the landscape and transmits this video in real-time to the ground station, in our case a laptop. The AAV passes by four different phases, see Figure 11, while transmitting the video signal:

1) Phase A: The AAV is stationary on the ground and close to the laptop (the ground station). This takes place during the initialization and AAV preparation.
2) Phase B: The AAV is moving slowly and with close range to the laptop. This takes place when moving the AAV to the take-off runway.

TABLE I
RECEIVED VIDEO DURATION FOR TEMPORAL DISTORTION

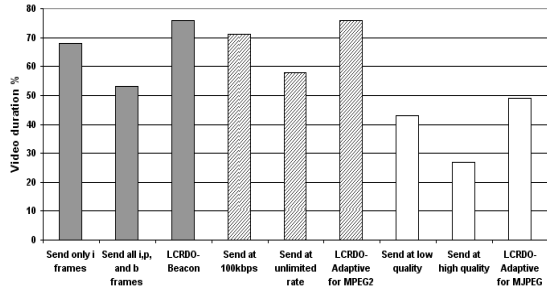| Experiment	video duration
1(a) Send only i frames	68 %
1(b) Send all i, p, and b frames	53 %
1(c) LCRDO-Beacon	76 %
2(a) Send at 100kbps	71 %
2(b) Send at unlimited rate	58 %
2(c) LCRDO-Adaptive for MPEG2	76 %
3(a) Send at low quality	43 %
3(b) Send at high quality	27 %
3(c) LCRDO-Adaptive for MJPEG	49 %

Fig. 12.   Received video duration for temporal distortion.

TABLE II
AVERAGE SSIM INDICES FOR SPATIAL DISTORTION

Experiment	Phases				Overall
	A	B	C	D	SSIM
1(a) Send only i frames	1	0.73	0.90	0.69	0.77
1(b) Send all i, p, and b frames	1	0.84	0.84	0.67	0.77
1(c) LCRDO-Beacon	1	0.68	0.73	0.79	0.78
2(a) Send at 100kbps	0.96	0.72	0.75	0.65	0.71
2(b) Send at unlimited rate	1	0.77	0.90	0.71	0.79
2(c) LCRDO-Adaptive MPEG2	1	0.84	0.79	0.67	0.76
3(a) Send at low quality	0.94	0.95	0.94	0.93	0.94
3(b) Send at high quality	1	1	1	1	1
3(c) LCRDO-Adaptive MJPEG	1	1	0.93	0.94	0.96

Fig. 13.   Average SSIM indices for spatial distortion.

3) Phase C: The AAV is moving relatively very fast and with moderate range to the laptop. This takes place at take-off and landing. In this case the camera view is changing rapidly.

4) Phase D: The AAV is moving relatively fast and far from the laptop. This takes place when the AAV is in the air.

For our experiments, we analyze both temporal and spatial distortion. For temporal distortion, we compare the video at the receiver/destination and the video at the transmitter/source with respect to video duration. For spatial distortion, we compare the SSIM index of 10 highest and 10 lowest spatially distorted video frames received at the destination. The frame selection is done manually by eye inspection. The number of frames selected from the flight phases A, B, C, and D are 2, 4, 4, and 10, respectively. The SSIM index is calculated for each frame with respect to the corresponding source frame using equation III.1. Then, the average, i.e. arithmetic mean, of SSIM indices for all the selected 20 frames is calculated for each case in each flight experiment. Table I and Figure 12 show the temporal distortion results for our experiments. For every experiment, the percentage of the received video duration is highest for case (c). Hence, we can conclude that a better optical flow of received video is observed when applying the LCRDO algorithms compared to the other two cases for each experiment. Therefore, the temporal distortion observed by the user is minimal in the LCRDO algorithms. This matches our observations during real-time field testing. In terms of spatial distortions, we observed that the average SSIM indices for case (a), (b), and (c) within each experiment are approximately equal, see Table II. We conclude that the average SSIM index is more dependent on the compression type compared to the transmission algorithm. Nevertheless,

spatial distortions in the RDO case are always less than when streaming with a low quality encoder, approaching the level of high quality encoding yet with much better temporal behavior. The average SSIM indices for the proposed RDO algorithms is summarized in Table II and Figure 13. The MJPEG/SMOKE codec outperforms MPEG2 codec in terms of its average SSIM index. This is due to inter-frame estimation performed in the MPEG2 decoder, which causes partially received frames to be viewed as distorted frames. By contrast, partially received frames are dropped in the MPJEG/SMOKE decoder, leading to higher temporal distortions instead. Finally, we conducted a flight experiment for the multiple unicast network topology. The two AAVs transmit two different video signals simultaneously to a common ground station (laptop) using the LCRDO-Adaptive for MJPEG algorithm. The main observation is that we can display both videos with acceptable optical flow. Successful reception of multiple unicast flows should open more possibilities for future work in building larger AAV networks that can transmit/receive videos to/from multiple destinations/sources. As discussed previously, any implementation of the more complex multiple unicast case should easily transfer into a multicast environment.

V. CONCLUSION

In this paper, we developed low complexity rate distortion optimized (LCRDO) and adaptive video streaming algorithms. These algorithms are applied to a real testbed called Horus consisting of a network of wirelessly connected AAVs and ground stations. Our experiments show that our developed LCRDO and adaptive videos streaming algorithm outperform conventional video streaming algorithms. The design of these algorithms take in consideration the bandwidth, computation

and power limitations of mobile cyberphysical systems. We provide comparison between the tested algorithms with respect to temporal and spatial distortion metrics.

REFERENCES

[1] Philo Juang, Hidekazu Oki, Yong Wang, Margaret Martonosi, Li shiuan Peh, and Daniel Rubenstein. Energy-Efficient Computing for Wildlife Tracking: Design Tradeoffs and Early Experiences with ZebraNet. In *Proc. of ACM (ASPLOS-X)*, pages 96–107, October 2002.

[2] P. A. Chou and Z. Miao. Rate-Distortion Optimized Streaming of Packetized Media. *IEEE Transaction on Multimedia*, May 2005.

[3] Ting Liu, Christopher M. Sadler, Pei Zhang, and Margaret Martonosi. Implementing Software on Resource-Constrained Mobile Sensors: Experiences with Impala and ZebraNet. In *Proc. of MobiSYS '04*, pages 256–269. ACM Press, 2004.

[4] Pei Zhang, Christopher M. Sadler, Stephen A. Lyon, and Margaret Martonosi. Hardware Design Experiences in ZebraNet. In *Proc. of SenSys '04*, November 2004.

[5] H. Zhou, X. Wang, Z. Liu, X. Zhao, Y. Ji, and S. Yamada. Qos-aware resource allocation for multicast service over vehicular networks. In *2016 8th International Conference on Wireless Communications Signal Processing (WCSP)*, pages 1–5, Oct 2016.

[6] Z. Fan, Y. Li, G. Shen, and C. C. K. Chan. Dynamic resource allocation for all-optical multicast based on sub-tree scheme in elastic optical networks. In *2016 Optical Fiber Communications Conference and Exhibition (OFC)*, pages 1–3, March 2016.

[7] Akshay Kumar, Ahmed Abdelhadi, and T. Charles Clancy. A delay efficient multiclass packet scheduler for heterogeneous M2M uplink. *IEEE MILCOM*, 2016.

[8] Akshay Kumar, Ahmed Abdelhadi, and T. Charles Clancy. An online delay efficient packet scheduler for M2M traffic in industrial automation. *IEEE Systems Conference*, 2016.

[9] Akshay Kumar, Ahmed Abdelhadi, and T. Charles Clancy. A delay optimal MAC and packet scheduler for heterogeneous M2M uplink. *CoRR*, abs/1606.06692, 2016.

[10] Ahmed Abdel-Hadi and Sriram Vishwanath. On multicast interference alignment in multihop systems. In *IEEE Information Theory Workshop 2010 (ITW 2010)*, 2010.

[11] J. Jose, A. Abdel-Hadi, P. Gupta, and S. Vishwanath. On the impact of mobility on multicast capacity of wireless networks. In *INFOCOM, 2010 Proceedings IEEE*, pages 1–5, March 2010.

[12] S. Gao and M. Tao. Energy-efficient resource allocation for multiple description coding based multicast services in ofdma networks. In *2016 IEEE/CIC International Conference on Communications in China (ICCC)*, pages 1–6, July 2016.

[13] Surachai Chieochan and Ekram Hossain. Downlink Media Streaming with Wireless Fountain Coding in wireline-cum-WiFi Networks. *Wirel. Commun. Mob. Comput.*, 12(17):1567–1579, December 2012.

[14] Ahmed Abdelhadi, Felipe Rechia, Arvind Narayanan, Thiago Teixeira, Ricardo Lent, Driss Benhaddou, Hyunwoo Lee, and T. Charles Clancy. Position Estimation of Robotic Mobile Nodes in Wireless Testbed using GENI. *CoRR*, abs/1511.08936, 2015.

[15] S. Chieochan and E. Hossain. Wireless Fountain Coding with IEEE 802.11e Block ACK for Media Streaming in Wireline-cum-WiFi Networks: A Performance Study. *IEEE Transactions on Mobile Computing*, 10(10):1416–1433, Oct 2011.

[16] S. Chieochan and E. Hossain. Network Coding for Unicast in a WiFi Hotspot: Promises, Challenges, and Testbed Implementation. *Comput. Netw.*, 56(12):2963–2980, August 2012.

[17] D. Agrawal, T. Bheemarjuna Reddy, C. Siva, and Ram Murthy. Robust Demand-Driven Video Multicast over Ad hoc Wireless Networks. In *Proc. of BroadNets '06*, October 2006.

[18] Z. Kbah and A. Abdelhadi. Resource allocation in cellular systems for applications with random parameters. In *2016 International Conference on Computing, Networking and Communications (ICNC)*, pages 1–5, Feb 2016.

[19] T. Erpek, A. Abdelhadi, and T. C. Clancy. Application-aware resource block and power allocation for LTE. In *2016 Annual IEEE Systems Conference (SysCon)*, pages 1–5, April 2016.

[20] R. Braden. Resource ReSerVation Protocol (RSVP) - Version 1 Functional Specification. 1997.

[21] S. Blake. An Architecture for Differentiated Services. 1998.

[22] K. Nichols. A Two-Bit Differentiated Services Architecture for the Internet. 1999.

[23] K. Nahrstedt. The QoS Broker. 1995.

[24] I. Jung, Insoon J., Youngjin Y., Hyeonsang E., and H. Yeom. Enhancing QoS and Energy Efficiency of Realtime Network Application on Smartphone Using Cloud Computing. In *IEEE Asia-Pacific Services Computing Conference (APSCC)*, 2011.

[25] Tellabs. Quality of Service in the Wireless Backhaul. 2012.

[26] N. Ahmed and H. Yan. Access control for MPEG video applications using neural network and simulated annealing. In *Mathematical Problems in Engineering*, 2004.

[27] J. Tournier, J. Babau, and V. Olive. Qinna, a Component-based QoS Architecture. In *Proceedings of the 8th International Conference on Component-Based Software Engineering*, 2005.

[28] G. Gorbil and I. Korpeoglu. Supporting QoS traffic at the network layer in multi-hop wireless mobile networks. In *Wireless Communications and Mobile Computing Conference (IWCMC)*, 2011.

[29] L. B. Le, E. Hossain, D. Niyato, and D. I. Kim. Mobility-aware admission control with qos guarantees in ofdma femtocell networks. In *2013 IEEE International Conference on Communications (ICC)*, pages 2217–2222, June 2013.

[30] L. B. Le, D. Niyato, E. Hossain, D. I. Kim, and D. T. Hoang. QoS-Aware and Energy-Efficient Resource Management in OFDMA Femtocells. *IEEE Transactions on Wireless Communications*, 12(1):180–194, January 2013.

[31] L. Chung. Energy efficiency of qos routing in multi-hop wireless networks. In *IEEE International Conference on Electro/Information Technology (EIT)*, 2010.

[32] M. Alasti, B. Neekzad, Jie H., and R. Vannithamby. Quality of service in WiMAX and LTE networks [Topics in Wireless Communications]. 2010.

[33] D. Niyato and E. Hossain. WIRELESS BROADBAND ACCESS: WIMAX AND BEYOND - Integration of WiMAX and WiFi: Optimal Pricing for Bandwidth Sharing. *IEEE Communications Magazine*, 45(5):140–146, May 2007.

[34] D. Fudenberg and J. Tirole. Nash equilibrium: multiple Nash equilibria, focal points, and Pareto optimality. In *MIT Press*, 1991.

[35] Mo Ghorbanzadeh, Ahmed Abdelhadi, and Charles Clancy. Utility functions and radio resource allocation. In *Cellular Communications Systems in Congested Environments*, pages 21–36. Springer, 2017.

[36] H. Kushner and P. Whiting. Convergence of proportional-fair sharing algorithms under general conditions. 2004.

[37] M. Andrews, K. Kumaran, K. Ramanan, A. Stolyar, P. Whiting, and R. Vijayakumar. Providing quality of service over a shared wireless link. 2001.

[38] G. Tychogiorgos, A. Gkelias, and K. Leung. Utility proportional fairness in wireless networks. IEEE International Symposium on Personal, Indoor, and Mobile Radio Communications (PIMRC), 2012.

[39] M. Li, Z. Chen, and Y. Tan. A maxmin resource allocation approach for scalable video delivery over multiuser mimo-ofdm systems. In *IEEE International Symposium on Circuits and Systems (ISCAS)*, 2011.

[40] R. Prabhu and B. Daneshrad. An energy-efficient water-filling algorithm for ofdm systems. In *IEEE International Conference on Communications (ICC)*, 2010.

[41] T. Harks. Utility proportional fair bandwidth allocation: An optimization oriented approach. In *QoS-IP*, 2005.

[42] T. Nandagopal, T. Kim, X. Gao, and V. Bharghavan. Achieving mac layer fairness in wireless packet networks. In *Proceedings of the 6th annual International Conference on Mobile Computing and Networking (Mobicom)*, 2000.

[43] F. Kelly, A. Maulloo, and D. Tan. Rate control in communication networks: shadow prices, proportional fairness and stability. In *Journal of the Operational Research Society*, 1998.

[44] S. Low and D. Lapsley. Optimization flow control, i: Basic algorithm and convergence. 1999.

[45] A. Parekh and R. Gallager. A generalized processor sharing approach to flow control in integrated services networks: the single-node case. 1993.

[46] A. Demers, S. Keshav, and S. Shenker. Analysis and simulation of a fair queueing algorithm. 1989.

[47] R. Kurrle. Resource allocation for smart phones in 4g lte advanced carrier aggregation. Master Thesis, Virginia Tech, 2012.

[48] J. Lee, R. Mazumdar, and N. Shroff. Non-convex optimization and rate control for multi-class services in the internet. 2005.

[49] J. Lee, R. Mazumdar, and N. Shroff. Downlink power allocation for multi-class wireless systems. 2005.

[50] Ahmed Abdelhadi, Awais Khawar, and T Charles Clancy. Optimal downlink power allocation in cellular networks. *Physical Communication*, 17:1–14, 2015.

[51] S. Boyd and L. Vandenberghe. *Introduction to convex optimization with engineering applications*. Course Reader, 2001.

[52] Mo Ghorbanzadeh, Ahmed Abdelhadi, and Charles Clancy. Resource allocation architectures traffic and sensitivity analysis. In *Cellular Communications Systems in Congested Environments*, pages 93–116. Springer, 2017.

[53] M. Ghorbanzadeh, A. Abdelhadi, and C. Clancy. A Utility Proportional Fairness Approach for Resource Block Allocation in Cellular Networks. In *IEEE International Conference on Computing, Networking and Communications (ICNC)*, 2015.

[54] T. Erpek, A. Abdelhadi, and C. Clancy. An Optimal Application-Aware Resource Block Scheduling in LTE. In *IEEE International Conference on Computing, Networking and Communications (ICNC) Worshop CCS)*, 2015.

[55] Mo Ghorbanzadeh, Ahmed Abdelhadi, and Charles Clancy. Radio resource block allocation. In *Cellular Communications Systems in Congested Environments*, pages 117–146. Springer, 2017.

[56] Mo Ghorbanzadeh, Ahmed Abdelhadi, and Charles Clancy. *Book Summary*, pages 241–244. Springer, 2017.

[57] Mo Ghorbanzadeh, Ahmed Abdelhadi, and Charles Clancy. Delay-based backhaul modeling. In *Cellular Communications Systems in Congested Environments*, pages 179–240. Springer, 2017.

[58] Ahmed Abdelhadi and Haya Shajaiah. Optimal Resource Allocation for Smart Phones with Multiple Applications with MATLAB Instructions. 2016.

[59] Presidents Council of Advisors on Science Executive Office of the President and Technology (PCAST). Realizing the full potential of government-held spectrum to spur economic growth. 2012.

[60] S. Wilson and T. Fischetto. Coastline population trends in the united states: 1960 to 2008. In *U.S. Dept. of Commerce*, 2010.

[61] M. Richards, J. Scheer, and W. Holm. Principles of Modern Radar. 2010.

[62] Federal Communications Commission (FCC). In the matter of revision of parts 2 and 15 of the commissions rules to permit unlicensed national information infrastructure (U-NII) devices in the 5 GHz band. MO&O, ET Docket No. 03-122, June 2006.

[63] Federal Communications Commission. Proposal to Create a Citizen's Broadband Service in the 3550-3650 MHz band. 2012.

[64] Federal Communications Commission (FCC). Connecting America: The national broadband plan. Online, 2010.

[65] NTIA. An assessment of the near-term viability of accommodating wireless broadband systems in the 1675-1710 mhz, 1755-1780 mhz, 3500-3650 mhz, 4200-4220 mhz and 4380-4400 mhz bands. 2010.

[66] National Telecommunications and Information Administration (NTIA). Analysis and resolution of RF interference to radars operating in the band 2700-2900 MHz from broadband communication transmitters. Online, October 2012.

[67] Cotton M. and Dalke R. Spectrum occupancy measurements of the 3550-3650 megahertz maritime radar band near san diego, california. 2014.

[68] G. Tychogiorgos, A. Gkelias, and K. Leung. A New Distributed Optimization Framework for Hybrid Adhoc Networks. In *GLOBECOM Workshops*, 2011.

[69] G. Tychogiorgos, A. Gkelias, and K. Leung. Towards a Fair Non-convex Resource Allocation in Wireless Networks. In *IEEE International Symposium on Personal, Indoor, and Mobile Radio Communications (PIMRC)*, 2011.

[70] T. Jiang, L. Song, and Y. Zhang. Orthogonal frequency division multiple access fundamentals and applications. In *Auerbach Publications*, 2010.

[71] G. Yuan, X. Zhang, W. Wang, and Y. Yang. Carrier aggregation for LTE-advanced mobile communication systems. In *Communications Magazine, IEEE*, volume 48, pages 88–93, 2010.

[72] Yuanye Wang, K.I. Pedersen, P.E. Mogensen, and T.B. Sorensen. Resource allocation considerations for multi-carrier lte-advanced systems operating in backward compatible mode. In *Personal, Indoor and Mobile Radio Communications, 2009 IEEE 20th International Symposium on*, pages 370–374, 2009.

[73] H. Shajaiah, A. Abdelhadi, and C. Clancy. Utility proportional fairness resource allocation with carrier aggregation in 4g-lte. In *IEEE Military Communications Conference (MILCOM)*, 2013.

[74] H. Shajaiah, A. Abdelhadi, and C. Clancy. Multi-application resource allocation with users discrimination in cellular networks. In *IEEE nternational Symposium on Personal, Indoor and Mobile Radio Communications (PIMRC)*, 2014.

[75] A. Abdelhadi and C. Clancy. An optimal resource allocation with joint carrier aggregation in 4G-LTE. In *Computing, Networking and Communications (ICNC), 2015 International Conference on*, pages 138–142, Feb 2015.

[76] Haya Shajaiah, Ahmed Abdelhadi, and T. Charles Clancy. An efficient multi-carrier resource allocation with user discrimination framework for 5g wireless systems. *Springer International Journal of Wireless Information Networks*, 22(4):345–356, 2015.

[77] Ahmed Abdelhadi and Haya Shajaiah. Application-Aware Resource Allocation with Carrier Aggregation using MATLAB. 2016.

[78] H. Shajaiah, A. Abdelhadi, and C. Clancy. A price selective centralized algorithm for resource allocation with carrier aggregation in lte cellular networks. In *2015 IEEE Wireless Communications and Networking Conference (WCNC)*, pages 813–818, March 2015.

[79] Haya Shajaiah, Ahmed Abdelhadi, and Charles Clancy. Spectrum sharing approach between radar and communication systems and its impact on radar's detectable target parameters. In *Vehicular Technology Conference (VTC Spring), 2015 IEEE 81st*, pages 1–6, May 2015.

[80] A. Lackpour, M. Luddy, and J. Winters. Overview of interference mitigation techniques between wimax networks and ground based radar. 2011.

[81] F. Sanders, J. Carrol, G. Sanders, and R. Sole. Effects of radar interference on lte base station receiver performance. 2013.

[82] Michael P. Fitz, Thomas R. Halford, Iftekhar Hossain, and Scott W. Enserink. Towards Simultaneous Radar and Spectral Sensing. In *IEEE International Symposium on Dynamic Spectrum Access Networks (DYSPAN)*, pages 15–19, April 2014.

[83] Z. Khan, J. J. Lehtomaki, R. Vuohtoniemi, E. Hossain, and L. A. Dasilva. On opportunistic spectrum access in radar bands: Lessons learned from measurement of weather radar signals. *IEEE Wireless Communications*, 23(3):40–48, June 2016.

[84] M. Ghorbanzadeh, A. Abdelhadi, and C. Clancy. A Utility Proportional Fairness Bandwidth Allocation in Radar-Coexistent Cellular Networks. In *Military Communications Conference (MILCOM)*, 2014.

[85] A. Abdelhadi and T. C. Clancy. Network MIMO with partial cooperation between radar and cellular systems. In *2016 International Conference on Computing, Networking and Communications (ICNC)*, pages 1–5, Feb 2016.

[86] Mo Ghorbanzadeh, Ahmed Abdelhadi, and Charles Clancy. Spectrum-shared resource allocation. In *Cellular Communications Systems in Congested Environments*, pages 147–178. Springer, 2017.

[87] Via EPIA Nano-ITX, http://www.via.com.tw/en/products/embedded/ProductDetail.jsp- motherboard -id-470.

[88] CM9-GP: 802.11 a/b/g 108Mbps wifi mini-PCI module, MB42/AR5213A+AR5112, http://www.unex.com.tw/product/cm9 -gp.

[89] XBee-PRO DigiMesh 900 Mesh RF Modules, http://www.digi.com/products/wireless/zigbee-mesh/xbee-digimesh-900.

[90] UAV v2 Development Platform, http://www.sparkfun.com/datasheets /GPS/GPSUAV2-Manual-v29.pdf.

[91] 20 Channel EM-406A SiRF III Receiver with Antenna, http://www.sparkfun.com/datasheets/GPS/EM-406A-UserManual.

[92] Hitec Eclipse 7 7-Channel FM Transmitter/Spectra, http://www.scribd.com/doc/16070675/Hitec-Eclipse-7-Transmitter-Manual.

[93] HS-322 Deluxe Standard Servo, http://www.hobby-lobby.com/hs-322-standard-servo-2786-prd1.htm.

[94] Hacker Brushless A40-10L, http://www.aero-model.com/Hacker-Brushless-A40-10L.aspx.

[95] Z. Wang, A. Bovik, H. Sheikh, and E. Simoncelli. Image quality assessment: From error visibility to structural similarity. *IEEE Transactions on Image Processing*, pages 600–612, Apr. 2004.

[96] The Click Modular Router Project, http://read.cs.ucla.edu/click/click.

[97] GStreamer: open source multimedia framework, http://gstreamer.freedesktop.org/.

[98] Smoke Encoder, http://www.flumotion.net/doc/flumotion/manual/en/0.6.0/html/.

[99] Austin RC, http://www.austinrc.org/index.html.